hep-ph/9908464 25 Aug 1999

LU TP 99–13
CERN–TH/99–240
MAN/HEP/99/3
MC-TH-99/09
August 1999

Hard Colour Singlet Exchange at the Tevatron

Brian Cox
*Dept. of Physics and Astronomy, University of Manchester
Manchester M13 9PL, England
coxb@mail.desy.de

Jeff Forshaw[1]
Theory Division, CERN
1211 Geneva 23, Switzerland
forshaw@mail.cern.ch

Leif Lönnblad
Dept. of Theoretical Physics 2, Sölvegatan 14A
S-223 62 Lund, Sweden
leif@thep.lu.se

Abstract

We have performed a detailed phenomenological investigation of the hard colour singlet exchange process which is observed at the Tevatron in events which have a large rapidity gap between outgoing jets. We include the effects of multiple interactions to obtain a prediction for the gap survival factor. Comparing the data on the fraction of gap events with the prediction from BFKL pomeron exchange we find agreement provided that a constant value of α_s is used in the BFKL calculation. Moreover, the value of α_s is in line with that extracted from measurements made at HERA.

[1]On leave of absence from *

1 Introduction

Diffractive scattering has yet to be understood within the framework of QCD. The problem arises because diffractive processes usually depend upon physics at distances which are not small on the scale typical of strong interactions.

Diffractive events are often selected by looking for regions in rapidity which are void of activity. Rapidity gaps are correlated with diffractive scattering since diffraction takes place in the limit where the invariant centre-of-mass energy is much larger than any other invariant. The challenge is to understand the gap producing mechanism using QCD.

Figure 1 shows a generic rapidity gap event and serves to set our notation. The final state is composed of two clusters, X and Y, which are separated in rapidity. As usual the Mandelstam variables are labelled s and t.

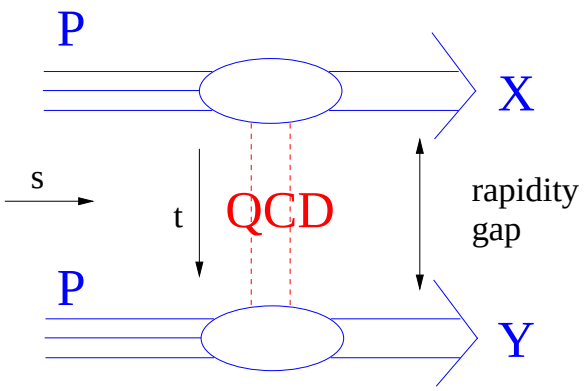

Figure 1: A generic rapidity gap process.

Typically, the gaps are produced with little or no momentum transfer, t, and this makes life difficult for those wanting to employ the tools of perturbative QCD. However, it is possible to squeeze the gap producing mechanism to short distances: one looks for gap events in which a large momentum is transferred across the gap, i.e. $-t \gg \Lambda^2_{\rm QCD}$ [1,2].

Experiments at the Tevatron and at HERA have already examined a variety of these large t diffractive processes, the most inclusive of which is the double dissociation process $\gamma p \to X\,Y$ which has been studied at HERA [3].[2] The gaps-between-jets process, in which systems X and Y are each required to contain at least one jet, have been studied both at the Tevatron [4–7] and at HERA [8,9]. Additionally, the vector meson production process, $\gamma p \to V\,Y$, in which the system X is a single vector meson, V, has been measured at HERA [10, 11].

[2] At HERA system X is the product of the photon dissociation and system Y is the product of the proton dissociation.

Theoretically, the presence of a large momentum transfer across the gap supports the use of perturbative QCD [12]. The non-perturbative physics can be factorised into the usual parton density functions which can then be convoluted with the hard partonic scattering subprocess to determine the physical cross-section. The hard scattering subprocess can be calculated to an accuracy where all leading logarithms in energy, i.e. all terms $\sim \alpha_s^n \ln^n(s/|t|)$, are summed up using the formalism of BFKL [13]. Calculations have been performed for all of the above processes to leading logarithmic accuracy, see [14] for a recent summary.

In this paper, we wish to examine the Tevatron data on the gaps-between-jets process. We perform a detailed analysis of these data at 630 GeV and 1800 GeV and are drawn to conclude that the data are fully consistent with the leading logarithmic calculation of BFKL providing one fixes the strong coupling. This conclusion is consistent with that which can also be drawn from the HERA data collected to date. In our study, we pay particular attention to the issue of gap survival: we use PYTHIA to model the underlying event [15]. We consider observables at both the parton and hadron level.

The theoretical calculation

We start by explaining how we perform our theoretical calculations. We use the hard partonic subprocess first calculated in [2]:

$$\frac{d\sigma(qq\to qq)}{dt} = \left(\frac{\alpha_s C_F}{\pi}\right)^4 \frac{16\pi^3}{(N_c^2-1)^2}\frac{1}{t^2}\left[\int d\nu \frac{\nu^2}{(\nu^2+1/4)^2} \mathrm{e}^{\omega(\nu)y}\right]^2 \tag{1}$$

where the leading logarithm BFKL kernel is

$$\omega(\nu) = 2\frac{C_A\alpha_s}{\pi}\mathrm{Re}[\psi(1)-\psi(1/2+i\nu)] \tag{2}$$

and

$$y = \Delta\eta = \ln\left(\frac{\hat{s}}{-t}\right). \tag{3}$$

To this level of accuracy, the jets have equal and opposite transverse momenta, $p_T^2 = -t$. Throughout this paper we evaluate the right-hand-side of (1) without approximation although we do note that, in the limit $\Delta\eta \gg 1$, it simplifies to

$$\frac{d\sigma(qq\to qq)}{dt} \approx (C_F\alpha_s)^4 \frac{2\pi^3}{t^2}\frac{\exp(2\omega_0 y)}{(7\alpha_s C_A\zeta(3)y)^3} \tag{4}$$

where $\omega_0 = \omega(0) = C_A(4\ln 2/\pi)\alpha_s$. The gluon-quark and gluon-gluon subprocesses are the same as the quark-quark subprocess, up to colour factors, and so we can

write the parton level cross-section for the gaps-between-jets process as

$$\frac{d\sigma(h_1\ h_2 \to X\ Y)}{dx_1 dx_2 dt} = \left(\frac{81}{16} g_1(x_1,\mu^2) + \Sigma_1(x_1,\mu^2)\right)\left(\frac{81}{16} g_2(x_2,\mu^2) + \Sigma_2(x_2,\mu^2)\right) \frac{d\sigma(qq \to qq)}{dt} \tag{5}$$

where $g_i(x_i,\mu^2)$ is the gluon parton density function for hadron i and $\Sigma_i(x_i,\mu^2)$ is the sum over all quark and antiquark density functions for hadron i. These sub-processes have been coded into HERWIG [16,17] thereby allowing one to compute the likely corrections due to parton showering and hadronisation. We use a particular version of HERWIG which includes the BFKL subprocesses obtained using (1) without approximation [18].[3] Subsequently we take the factorisation scale $\mu^2 = -t$ (in the region of interest, $s \gg -t$, this is a very good approximation to the value chosen in HERWIG). We have used both CTEQ2M and CTEQ3M parton distribution functions [19,20], and have found the differences to be very small.

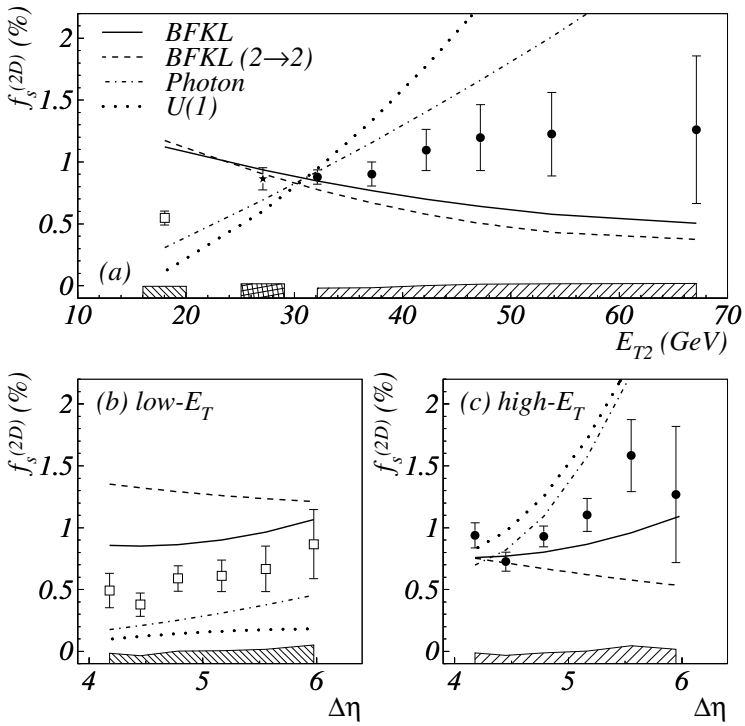

Figure 2: DØ data compared with a BFKL calculation. Plot from [5].

[3]The code can be obtained on request from `coxb@mail.desy.de`.

DØ data versus the BFKL pomeron

Let us now summarise the situation to date. Figure 2 shows the DØ data compared to a BFKL calculation. What is shown is the fraction of all dijet events in which the central region of the detector $|\eta| < 1$ is devoid of hadronic activity (see later for a more detailed explanation of the DØ selection cuts) as a function of the transverse energy of the lower E_T jet, E_{T2}, and the separation in rapidity of the jets, $\Delta\eta$. The CDF data at 1800 GeV do not go down to such low values of E_T and are consistent with a flat E_T distribution.

The BFKL curve is quite clearly excluded by the data. However, it should be understood that this curve was generated using the default settings in HERWIG [17]. In particular, this means that the asymptotic cross-section of (4) was used with a fixed value of $\omega_0 = 0.3$ in the exponent and a fixed value of $\alpha_s = 0.25$ in the denominator, whilst the α_s^4 prefactor was allowed to run with $-t$ according to the two-loop beta function. These settings are specific to the BFKL subprocess, in all other subprocesses the HERWIG default is to use the two-loop running coupling. The falling of the BFKL curve with increasing E_{T2} is driven by the running of the coupling in the pre-factor since the gap fraction goes like $\sim \alpha_s^4/\alpha_s^2$.

Now, to leading logarithmic accuracy α_s is simply an unknown parameter. Higher order corrections will indeed cause the coupling to run, however it is not clear how this should be done in a consistent way. In this paper we restrict ourselves to the leading logarithmic approximation and treat the coupling as a free parameter. Moreover, we are guided by recent HERA data on the double dissociation process [3] which can be described by the leading logarithmic BFKL formalism with a fixed strong coupling, $\alpha_s = 0.17$. We also note that a fixed coupling constant was needed in order to explain the high-t data on $p\bar{p}$ elastic scattering via three gluon exchange [21]. Furthermore, NLO corrections suggest a fixed value for the leading eigenvalue of the BFKL equation, $\omega(0)$, [22] which in turn suggests the use of a fixed coupling in the LLA kernel, i.e. in equation (2).

Underlying events and gap survival

So far we have said nothing about the possibility that gaps produced by the colour singlet exchange might be filled in as a consequence of secondary interactions between the colliding hadrons. The possibility that gaps do not survive formally invalidates the factorisation of the cross-section which we assumed in the previous sub-section. However, there are fairly good reasons (as we shall see in the next section) for expecting the effect to enter as a multiplicative 'gap survival' factor, $\mathcal{S}$, which specifies the probability that a gap produced at the hard scatter level survives to the hadron level. Note that we do expect $\mathcal{S}$ to vary with the centre-

of-mass energy of the colliding beams: as the centre-of-mass energy increases the corresponding proliferation of low-x partons makes a secondary partonic interaction more likely.

In the next section we shall use PYTHIA to extract the gap survival factors relevant to the Tevatron operating at 1800 GeV, at 630 GeV and for HERA at a fixed γp energy of 200 GeV. We will then use these factors to correct our cross-sections for processes involving gaps, i.e.

$$\frac{d\sigma(h_1\ h_2 \to X\ Y)}{dx_1 dx_2 dt} \to \mathcal{S}\frac{d\sigma(h_1\ h_2 \to X\ Y)}{dx_1 dx_2 dt}, \tag{6}$$

where $\mathcal{S}$ is the fraction of gap events which survive after including the effect of the underlying event as modelled in PYTHIA.

2 Gap Survival and Multiple Interactions

To investigate the gap survival probabilities we use a model for multiple interactions available in the PYTHIA program. Here the probability to have several parton–parton interactions in the same collision is modelled using perturbative QCD. For a given hard parton–parton scattering there is a probability of having additional scatterings given by the parton densities and the usual LO $2 \to 2$ matrix elements. The matrix elements are divergent for $p_\perp \to 0$ and are regulated by replacing the $1/p_\perp^4$ pole with $1/(p_\perp^2 + p_{\perp 0}^2)^2$ and using $p_\perp^2 + p_{\perp 0}^2$ as argument in α_s rather than just $p_\perp^2$. The value of $p_{\perp 0}$ varies with collision energy, $E_{\rm cm}$, and we have used the default behaviour: $p_{\perp 0} = (E_{\rm cm}/(1\text{TeV}))^{0.16} \cdot 2.1$ GeV.

The probability for additional interactions is not fixed but varies according to an impact-parameter picture, where central collisions are more likely to have multiple interactions. The partons in the proton are assumed to be distributed according to a double-gaussian as described in [15, 23]. There are several parameters in this model and we have used the default setting for each.[4] This is adequate for the accuracy required here but it should be noted that the parameters have not been tuned to Tevatron data.

Hard BFKL pomeron exchange has not been implemented in PYTHIA yet, but we can investigate the effects of multiple interactions on the gap survival probabilities in general by looking at high-t photon exchange. In Figure 3 and Figure 4 we show the gap fraction in photon exchange events at 1800 GeV with (mi4) and without (mi0) multiple interactions and, as expected, the probability for a gap introduced by the colourless photon scattering is greatly reduced in the presence of multiple

[4] Setting the switch `MSTP(82)=4` in PYTHIA, with everything else default, will give the model as we have used it.

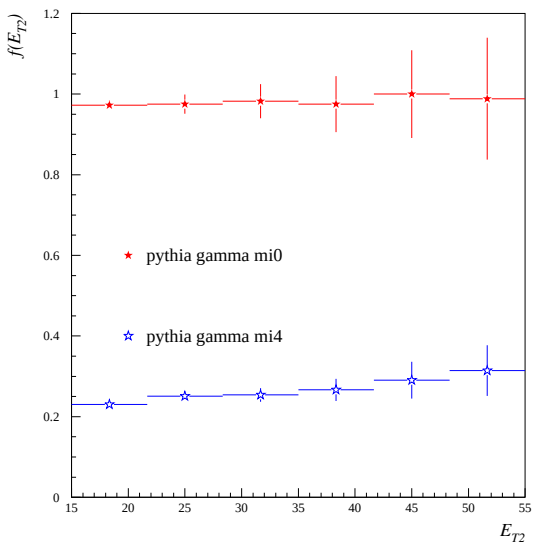

Figure 3: Gap fraction in photon exchange events at 1800 GeV with/without MI's: E_{T2} spectrum

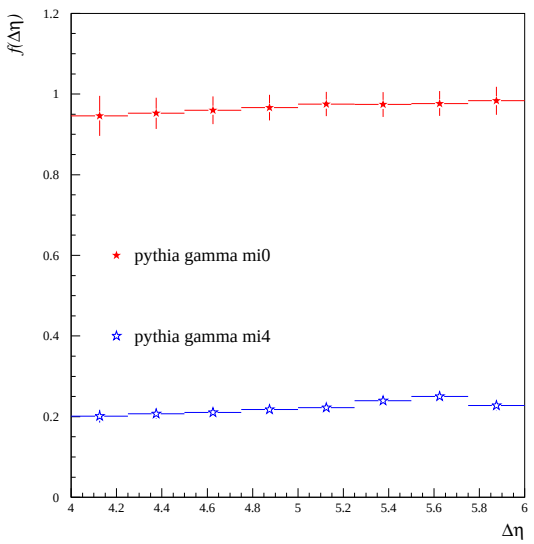

Figure 4: Gap fraction in photon exchange events at 1800 GeV with/without MI's: $\Delta\eta$ spectrum

interactions. The reason is that any additional scattering is likely to be a colourful one, destroying the gap. Thus we find the gap survival probability to be a simple multiplicative factor almost independent of the gap size and E_T although varying with the total collision energy. Figure 5 shows the effect of multiple interactions at the lower energy of 630 GeV.

In Figure 6 we show the effect in γp interactions at 200 GeV, as is relevant for HERA. In PYTHIA the procedure for generating these γp events requires some care. The cross-section is divided into three parts: direct, anomalous and VMD. Direct interactions, where the photon couples directly to the hard interaction, are not present in gamma exchange. Anomalous processes are resolved ones where the evolution from the photon is purely perturbative, while VMD are resolved processes where the photon has fluctuated into a vector meson state. Multiple interactions are only included in the latter processes, which is why the gap survival probability is much higher than in the hadron-hadron case. For γp we also use a simpler approach to multiple interactions, with an impact-parameter-independent probability for secondary scatterings since for this option there exists a set of tuned parameters [24] which we have used in the generation. The gap fraction after including multiple interactions is labelled 'mi1' in Figure 6.

In summary, we find $\mathcal{S}(1800\ \text{GeV}) = 22\%$, $\mathcal{S}(630\ \text{GeV}) = 35\%$ and $\mathcal{S}(\text{HERA}) = 67\%$.

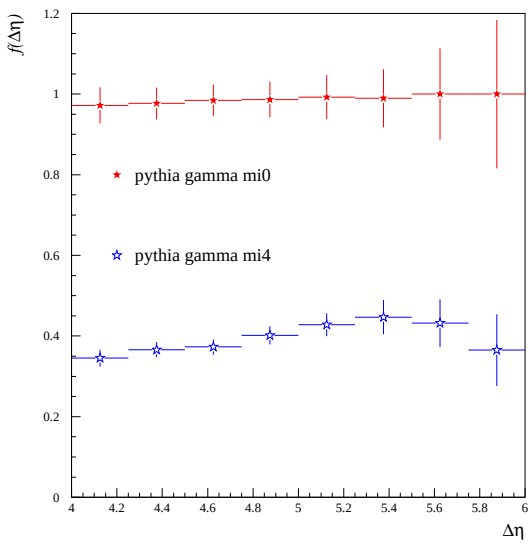

Figure 5: Gap fraction in photon exchange events at 630 GeV with/without MI's

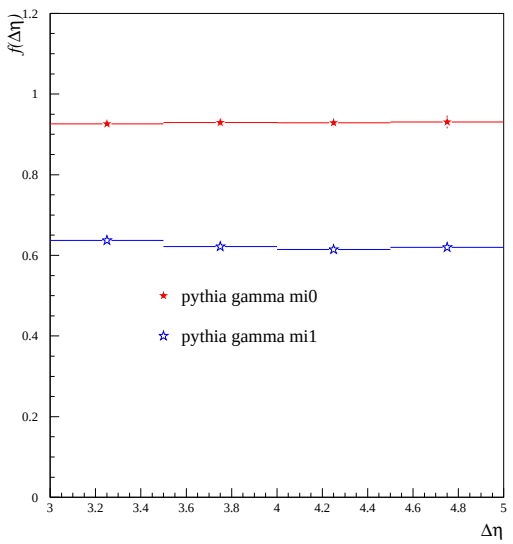

Figure 6: Gap fraction in photon exchange events at HERA with/without MI's

Note that requiring a large rapidity gap not only selects events with colour-singlet exchange in general, but in particular events with colour-singlet exchange without additional interactions.

Multiple interactions also give rise to the so-called jet pedestal and underlying event effects. This means that the jets measured in hadron-hadron collisions cannot be compared directly to e.g. predictions from fixed order perturbation theory. In Figure 7 we show jet profiles obtained from PYTHIA with and without multiple interactions (and with $|\delta\phi| < 0.7$). The proton remnant is at $\delta\eta > 0$. It is clear that multiple interactions introduce a jet pedestal of more than 1 GeV of E_T per unit rapidity. For comparison, also shown is the jet pedestal from HERWIG. We note that HERWIG predicts a greater amount of energy outside the jet cone than PYTHIA without multiple interactions. On the remnant side, $\delta\eta > 0$, the difference is accounted for by different treatments of the remnant (running HERWIG with `IOPREM=0` reproduces the PYTHIA result). However, on the gap side, $\delta\eta < 0$, the large difference is not so easy to explain. HERWIG does use a larger coupling than PYTHIA (see later), although this is not enough to account for the differences. The disagreement could be related to the differences in treatment of QCD coherence. Coherence in HERWIG is achieved by ordering emissions in the parton cascades in angle, while in PYTHIA the ordering is in virtuality with an additional angular constraint. The double ordering in PYTHIA reduces the emission probability and

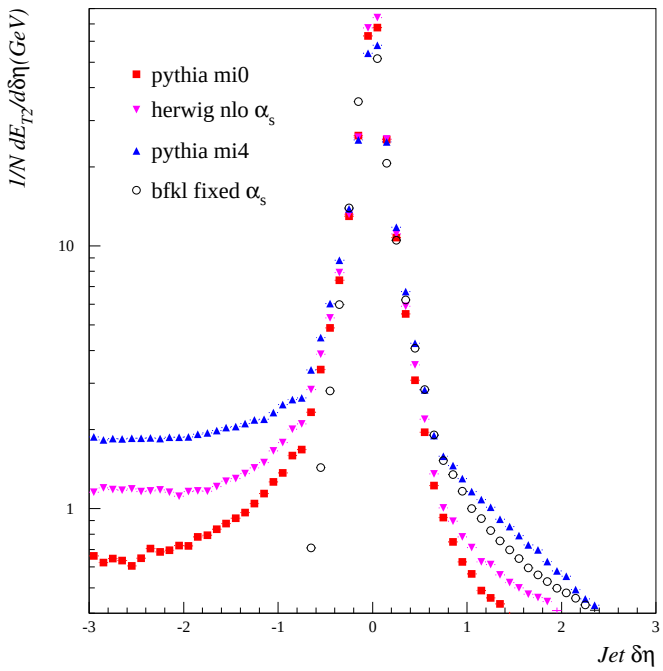

Figure 7: Jet η profiles

the fact that we are looking at jets at large rapidity (small angles) may enhance this effect. We have checked that relaxing the angular constraint in PYTHIA increases the E_T-flow on the gap side by $\approx 20\%$, although this needs to be studied further before firm conclusions can be made. Fortunately, as we shall see, it is likely that these differences mostly influence the overall normalisation of the gap fraction. However, it is important that these jet shapes are thoroughly confronted with data before precise estimates of the hadronisation corrections can be made.

In the DØ jet measurements the excess E_T from the underlying event is taken into account by correcting the jet E_T using data. In particular, the correction is determined by looking at the E_T in regions away from the jets. The correctness of this subtraction is also supported by a study of minimum bias events. The bottom line is that DØ subtract around 1 GeV from the E_T of each reconstructed jet [25]. In particular, in the gap fraction measurement, this subtraction is performed for all jets, including those in gap events. But, as we already pointed out, requiring a large rapidity gap also selects events without multiple interactions, where the jet pedestal is absent, or at least much smaller. Now, 1 GeV may seem like a small correction when we are looking at jets of $E_T = 18$ GeV or larger, but recall that the E_T spectrum is very steeply falling: typically it falls faster than $1/E_T^4$.

The correction may therefore be as large as 30% for $E_T = 18$ GeV, while for $E_T > 50$ GeV it will be less than 10%. Looking at Figure 2 we can roughly undo the erroneous correction of the jets in the gap events. The lowest E_T bin would then be increased a factor $(19/18)^4 \approx 1.24$ while the other points would be less affected. The increase of the gap fraction with increasing E_T then becomes less pronounced.

3 Results

Cross-sections at the parton and hadron level

In this section we show our results for jet cross-sections. Specifically, we work at 1800 GeV centre-of-mass energy and make the same analysis cuts as the DØ collaboration [5]. Jets are found using a cone algorithm [26, 27] with cone radius 0.7 and the `OVLIM` parameter set to 0.5. The inclusive dijet sample is defined by the following cuts:

- $|\eta_1|, |\eta_2| > 1.9$, i.e. jets are forward or backward
- $\eta_1 \eta_2 < 0$, i.e. opposite side jets
- $E_{T2} > 15$ GeV
- $\Delta\eta > 4$, i.e. jets are far apart in rapidity.

The sub-sample of gap events is obtained by employing the further cut that there be no particles emitted in the central region $|\eta| < 1$ with energy greater than 300 MeV. The CDF collaboration have performed a similar analysis [7] and we comment on their data wherever relevant. CDF use the same selection criteria as DØ except that they chose $1.8 < |\eta_{1,2}| < 3.5$, $E_{T2} > 20$ GeV for the 1800 GeV sample and $E_{T2} > 8$ GeV for the 630 GeV sample, and they make no further cut on the jet separation.[5]

We note that observables like the fraction of gap events to all events (the so-called gap fraction) are strictly not infrared safe. The definition of a gap event requires the specification of some threshold energy. Particles emitted into the gap with energy below this threshold by definition do not spoil the gap. In theoretical calculations this leads to logarithms in the infrared scale which formally diverge as the threshold is taken to zero. Thus theoretical predictions based on perturbation theory are in principle unstable as the threshold is lowered. One way to avoid this problem is to define a 'gap' to be an interval in rapidity which does not contain

[5] Strictly speaking we should set `OVLIM=0.75` when comparing to CDF data. However, the effect of implementing this change is negligible.

any jets above some E_T which is perturbatively large. However, the CDF and DØ gap samples are defined in such a way as to greatly reduce the sensitivity to the threshold energy. By insisting that the gap be a strip of width at least 2 units in rapidity centred on $\eta = 0$ and by forcing the jets to be at $\eta > 1.9$ the majority of events have gaps which do not encroach too closely to the edge of the jets. As a result, any soft radiation tends not to be emitted into the gap (it is localised around the leading parton). The problem would have been more acute if the gap sample had been defined by insisting that no particles be emitted (above the threshold) between the edges of the jet cones. This latter protocol has been used by the HERA experiments and should lead to results which depend significantly upon the threshold energy. We have explicitly checked that our results for the Tevatron do not change significantly as the threshold energy is varied from 0 MeV to 300 MeV.

In all cases results labelled 'bfkl fixed α_s' represent the cross-sections obtained using only the $2 \to 2$ hard subprocess cross-section of (1) with $\alpha_s = 0.17$; the value hinted at by the HERA data. Those labelled with 'bfkl running α_s' are obtained using the running coupling with the two-loop beta function ($\Lambda^{(5)}_{\rm QCD} = 200$ MeV) in the α_s^4 prefactor whilst keeping a fixed coupling, $\alpha_s = 0.17$, in the evaluation of $\omega(\nu)$. The parton showering and hadronisation are determined by the usual HERWIG defaults. Note that we have not yet corrected the BFKL data by the gap survival factor determined earlier.

All other results are cross-sections for the non-BFKL $2 \to 2$ subprocesses, i.e. they correspond to the usual QCD non-colour-singlet exchange subprocesses. More specifically: curves labelled 'HERWIG lo' are generated by HERWIG with a one-loop running coupling ($\Lambda^{(5)}_{\rm QCD} = 362$ MeV) whilst those labelled 'HERWIG nlo' are the HERWIG default curves obtained using a two-loop running coupling ($\Lambda^{(5)}_{\rm QCD} \approx 200$ MeV); similarly the PYTHIA curves are generated without multiple interactions ('mi0') or with multiple interactions ('mi4') and correspond to a one-loop running coupling with $\Lambda_{\rm QCD}$ determined by the value used in fitting the chosen parton density functions ($\Lambda^{(5)}_{\rm QCD} \approx 200$ MeV when using CTEQ2M). The $\Lambda_{\rm QCD}$ values quoted are the ones used to generate the parton level theory curves shown on some of the plots and, at two loop, are quoted in the $\overline{MS}$ scheme. The parton level theory curves are obtained from those bare $2 \to 2$ subprocess cross-sections which involve t-channel gluon exchange (t-channel quark exchange gives a negligible contribution), i.e. they do not include the effects of parton showering and hadronisation.

In Figure 8 we show the E_T spectrum of the lower E_T jet after hadronisation and parton showering. Note that there is a significant difference between the HERWIG and PYTHIA predictions. This is due to the different ways of running the coupling employed in the two programmes and the differences in fragmentation discussed earlier: data would help resolve the issue. Further sensitivity to the choice of α_s

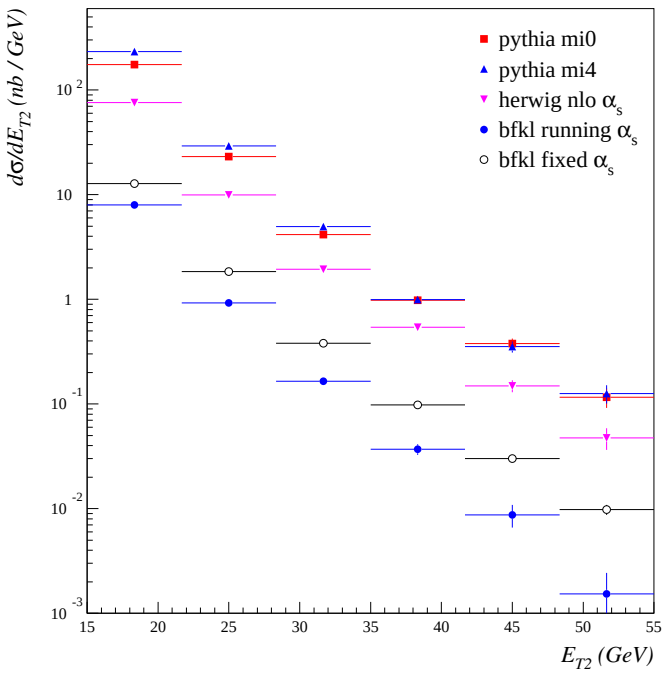

Figure 8: Cross-sections at the hadron level

(even in the non-BFKL case) can be seen in Figure 9, where we show the PYTHIA E_T spectrum of the lower E_T jet after hadronisation and parton showering but without multiple interactions, and compare to the parton level theory predictions and to HERWIG. Hadronisation and parton showering corrections are clearly very significant in both the BFKL and non-BFKL data sets. We have also looked at the relative role of hadronisation and parton showering and find that each contributes significantly to the deviations from the parton level theory predictions.

In Figure 10 we compare the parton level theory curves to the parton level cross-sections obtained from Monte Carlo. These $\Delta\eta$ distributions are obtained for the 'low E_T' jet sample, i.e. for those jets in the range 15 GeV $< E_{T2} <$ 25 GeV. As well as providing a cross-check, they serve to illustrate the dominance of t-channel gluon exchange. This plot also illustrates the effect of insisting that $|\eta_1|$, $|\eta_2| > 1.9$. The fall of the curve at low $\Delta\eta$ is a result of the increasingly strong requirement that the incoming partons have nearly equal and opposite energies. As a result, in the absence of the $\Delta\eta > 4$ cut, these cross-sections would fall smoothly to zero at $\Delta\eta = 3.8$. This kinematic effect could be removed by relaxing the constraint that the gap be central, i.e. by allowing the whole dijet system to tilt. The fall off of the $\Delta\eta$ distribution at large $\Delta\eta$ is due to the decrease of the parton densities with

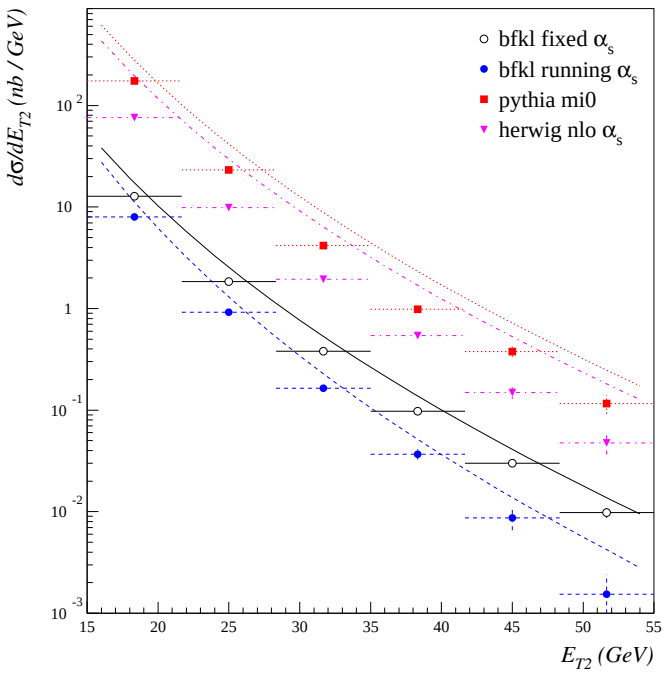

Figure 9: Comparison of Monte Carlo hadron level with theory parton level

increasing x.

Gap fractions

We now turn our attention to the gap fraction. This is the quantity usually measured by experiment. To construct the gap fraction we form the ratio

$$f = \frac{N^g_{BFKL} + N^g_{QCD}}{N_{BFKL} + N_{QCD}} \tag{7}$$

where N^g_{BFKL} is the number of events in the BFKL sample which also satisfy the gap cut, N^g_{QCD} is the number of events in the non-BFKL sample which satisfy the gap cut and the sum in the denominator is over all events in the dijet sample. The numerator is overwhelmingly dominated by BFKL events in all the plots we show.

In Figure 11 we show the hadron level gap fraction as a function of E_{T2}. All our gap fraction plots include the PYTHIA gap survival correction factor. The stars, corresponding to the ratio 'bfkl fixed α_s -1 GeV / pythia mi0', are the result of simulating the DØ jet correction procedure. We have subtracted 1 GeV from the BFKL jets and generated the non-BFKL sample by running PYTHIA

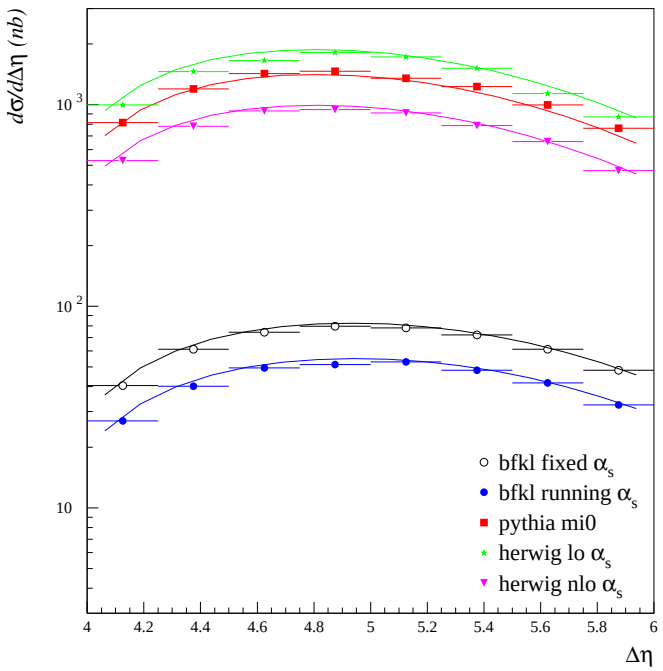

Figure 10: Low E_T events. Comparison of Monte Carlo parton level with theory parton level

without multiple interactions. Notice that these data points are in agreement with the the triangles labelled 'bfkl fixed α_s/ pythia mi4' which have been obtained without applying the jet correction to the BFKL sample and including multiple interaction effects in the non-BFKL sample. This agreement confirms our earlier claim that if one should want to correct for the affect of the underlying event (i.e. multiple interactions) then the correction can be approximated by a subtraction of 1 GeV from each jet. The squares in Figure 11 correspond to the gap fraction properly corrected for the underlying event, i.e. only the denominator (non-gap sample) has been corrected. Also shown in Figure 11 are comparisons with the ratio predicted using HERWIG to generate the non-BFKL sample and with a parton level theory calculation, labelled 'pythia mi0 parton' which was computed using the same prescription as PYTHIA for the running coupling (as detailed above).

The rise at low E_{T2} is mainly a result of including multiple interactions since, at low E_{T2}, the small amount of energy arising from the underlying event produced by secondary scatters enhances significantly the denominator (i.e. the full dijet sample) thereby reducing the gap fraction. Although we do note that a weaker rise, due to parton showering and hadronisation corrections, is still present in the

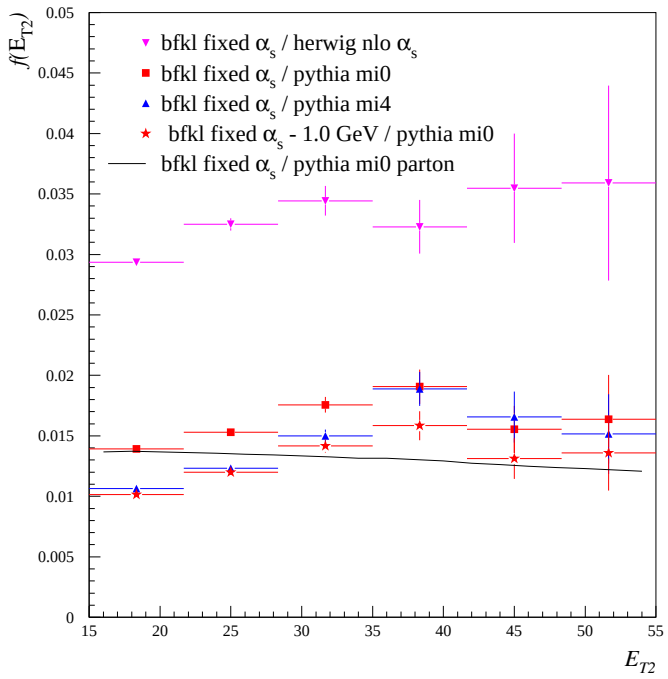

Figure 11: Gap fraction as a function of E_{T2}

HERWIG and PYTHIA mi0 samples.

Note also the decline of this rise of the gap fraction as E_{T2} increases. This effect is also present in the theory level curve (where it is seen as a falling distribution), even for fixed α_s, and reflects the tendency for the higher E_{T2} events to have a smaller $\Delta\eta$ due to the presence of the $(x_1 x_2 s/p_T^2)^{2\omega_0}$ factor in the numerator (the strong fall off of the parton density functions at large x means that larger p_T tends to occur without a corresponding increase in mean x). We note that we have used the BFKL formalism to sum the leading logarithms in the numerator of the gap fraction (supplemented with parton showering and hadronisation as determined by HERWIG) whilst using established Monte Carlos to predict the denominator. A strictly leading logarithmic calculation would also sum the leading logarithms in the denominator which could give rise to a factor in the denominator of $\sim (x_1 x_2 s/p_T^2)^{\omega_0}$. This physics has not yet been incorporated in HERWIG or PYTHIA and would have the effect of slowing down the fall of the E_T spectrum with increasing E_T.

Figure 12 shows the gap fraction as a function of $\Delta\eta$ for the low E_T sample and Figure 13 shows it for the high E_T sample. Notice that the effect of multiple interactions on the denominator of the gap fraction diminishes as E_{T2} increases.

Collectively, these gap fraction plots illustrate the uncertainty in theoretical pre-

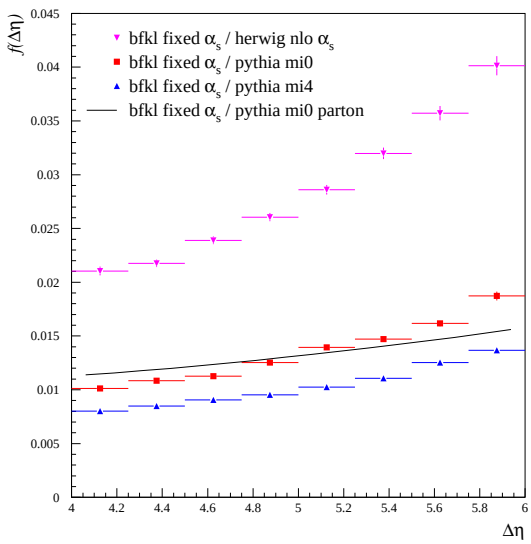

Figure 12: Gap fraction as a function of $\Delta\eta$ for $15 < E_{T2} < 25$ GeV

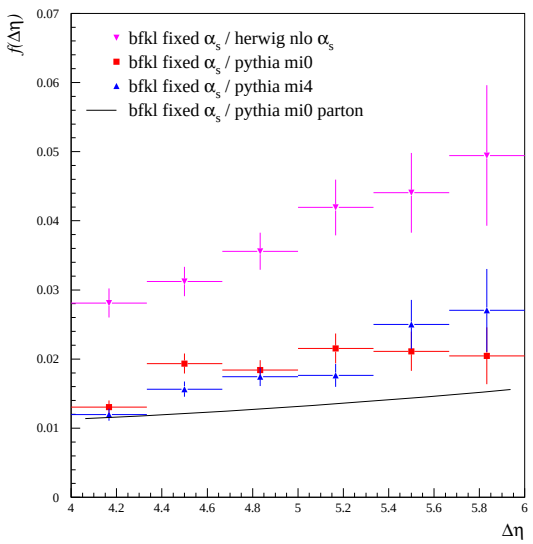

Figure 13: Gap fraction as a function of $\Delta\eta$ for $E_{T2} > 30$ GeV

diction even in the case of a particular ansatz for the BFKL behaviour: parton showering and hadronisation corrections are significant in computing the gap fraction.

Comparison to data

Now we come to our comparison with the DØ data. In order to make the comparison, we must first correct our gap events as discussed in Section 2, i.e. we subtract 1 GeV from each jet in the BFKL sample and generate the non-BFKL sample using PYTHIA without multiple interactions.

Figure 14 shows that after fixing the coupling and making the 1 GeV jet correction the open stars agree well with the data. Note that we have chosen to renormalise our results by a factor 0.6 in those plots where we compare to the DØ data. That this is a reasonable thing to do can be appreciated once it is realised that our results have not been fitted to the data and that the overall normalisation is acutely sensitive to the magnitude of α_s. Furthermore, the overall normalisation of the BFKL cross-section is uncertain since, within the leading logarithmic approximation, we are free to add any small constant to y in (1), i.e. the transformation $(s/p_T^2)^{2\omega} \to (s/(cp_T^2))^{2\omega}$ where c is some unknown constant ~ 1 is perfectly admissible. Given these points, we conclude that the DØ data are in agreement with the leading order BFKL result. We note that it is not possible to obtain agree-

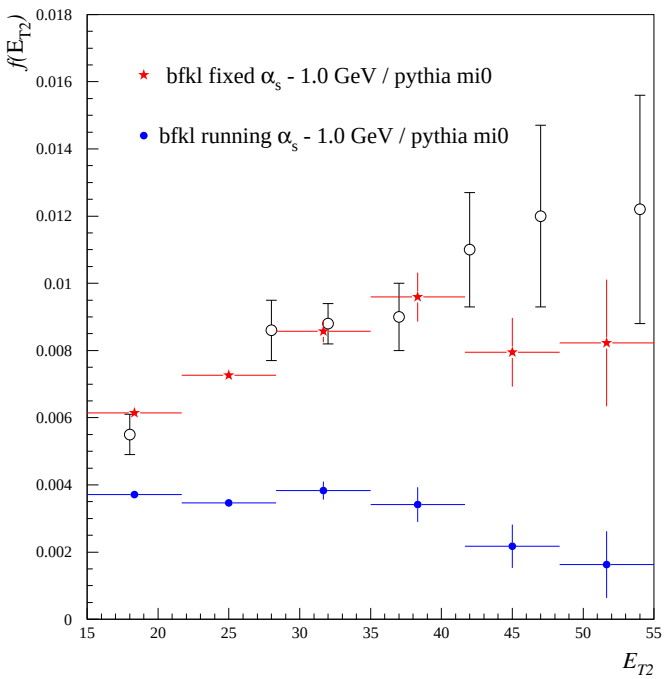

Figure 14: Gap fraction compared to the DØ data: E_{T2} spectrum.

ment with the data using a strong coupling which runs with the jet E_T, even after making the 1 GeV subtraction (the solid circles in Figure 14).

We could have chosen to use HERWIG to model the non-BFKL sample. In which case, the only significant effect, as illustrated in the preceding plots, would be a further overall shift in normalisation.

Figure 15 shows the $\Delta\eta$ distribution at low E_T and again the shape agrees well with the data. A similar story can be seen in Figure 16 which shows the $\Delta\eta$ distribution at high E_T. The data hint at the possibility that a renormalisation somewhat closer to unity (compared to the lower E_T case) of the BFKL prediction is needed in order to bring agreement with the data. However, as we mentioned earlier, summing the $\ln 1/x$ terms in the denominator will reduce the fall of the E_T spectrum as E_T increases and this would in turn lift the theory predictions in Figure 16.

In Figure 17 we show our prediction for the DØ gap fraction at 630 GeV compared to that at 1800 GeV. DØ has measured the ratio of the number of gap events at 630 GeV to the number at 1800 GeV and finds a value of 3.4 ± 1.2 [5].[6] This

[6] We note that the DØ ratio was actually obtained for $E_{T2} > 12$ GeV.

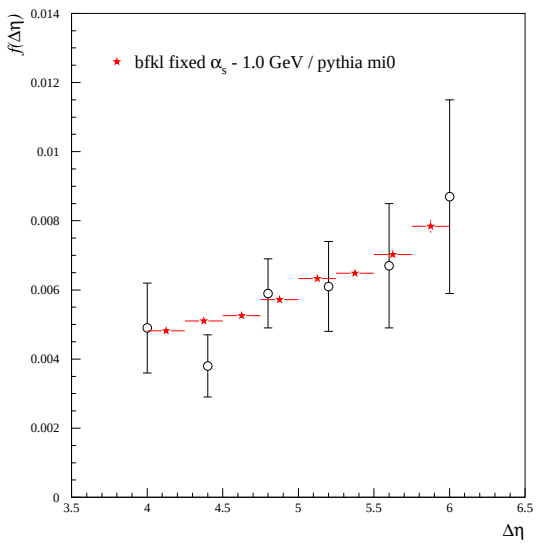

Figure 15: Gap fraction compared to the DØ data: $\Delta\eta$ spectrum at low E_T.

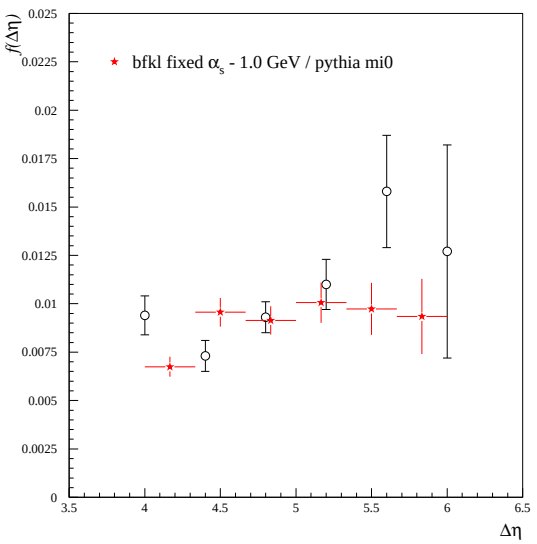

Figure 16: Gap fraction compared to the DØ data: $\Delta\eta$ spectrum at high E_T.

value can be seen to accord with the results shown in Figure 17. The data points represent our prediction whilst the solid line represents the parton level theory prediction. Clearly the effects of parton showering and hadronisation are very significant. The rise of the ratio illustrated in Figure 17 at large $\Delta\eta$ is understood. The restriction $x < 1$ forces the gap and non-gap cross-sections to fall to zero at some maximum $\Delta\eta$, $\Delta\eta_{\rm max}$. Now, the colour connection which exists between the jets in the non-gap sample drags the jets closer together in rapidity. This has a small effect away from $\Delta\eta_{\rm max}$ (since the $\Delta\eta$ spectrum is roughly flat) however as $\Delta\eta \to \Delta\eta_{\rm max}$ it leads to a more rapid vanishing of the non-gap cross-section than occurs in the gap cross-section. This effect, combined with the fact that $\Delta\eta_{\rm max}(630\ {\rm GeV}) < \Delta\eta_{\rm max}(1800\ {\rm GeV})$ leads to the rise illustrated in Figure 17. In Figure 18 we show explicitly the gap fraction at 630 GeV and one can see the large fragmentation corrections which occur as $\Delta\eta \to \Delta\eta_{\rm max}$. We note that CDF has also measured the ratio as a function of the momentum fractions of the final state jets (which are approximately equal to the momentum fractions of the incoming partons). They find a ratio of 2.4 ± 0.9 at fixed momentum fractions (the value is independent of the momentum fraction) [7]. The fall of the solid line (representing the tree level prediction) in Figure 17 arises since the 630 GeV data are at higher parton x than the corresponding 1800 GeV data and are consequently in a region where the gluon density falls off more sharply with increasing x than the quark distributions. Since the gluon is given more weight in the BFKL sample, this fall compensates the rise of the gap fraction due to the $\exp(2\omega_0 y)$ factor leading to a

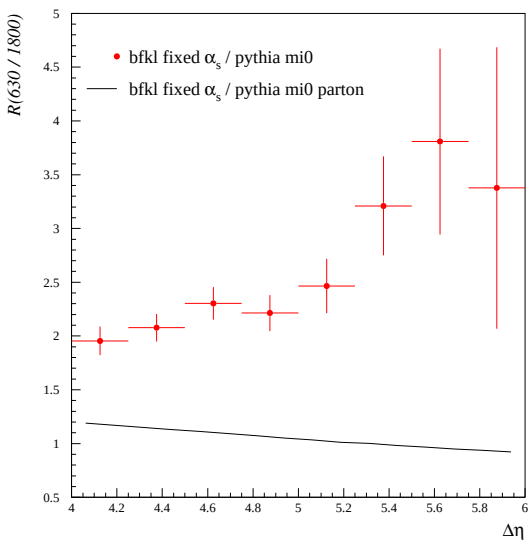

Figure 17: Ratio of the gap fraction at 630 GeV to that at 1800 GeV: $\Delta\eta$ spectrum for $E_{T2} > 15$ GeV.

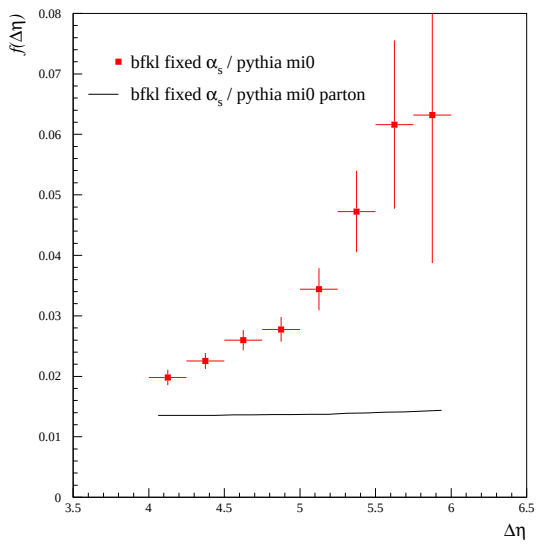

Figure 18: Gap fraction at 630 GeV: $\Delta\eta$ spectrum for $E_{T2} > 15$ GeV.

flatter $\Delta\eta$ distribution at 630 GeV than at 1800 GeV.

Finally, in Figure 19 we compare our results with the CDF data at 630 GeV and 1800 GeV: $\eta^* = \Delta\eta/2$. Note that CDF do not attempt to correct their jets to include the effect of an underlying event. In this plot, our theory points are obtained using a renormalisation factor of unity (compared to 0.6 in the DØ case) which is more in line with the normalisation suggested by the higher E_T DØ data and, as we have already discussed, is possibly expected on theoretical grounds after the inclusion of BFKL effects in the denominator of the gap fraction. We then find reasonable agreement with the data except at the larger values of η^* where we are quite unable to explain a fall in the η^* distribution. Recall however that DØ do not see a fall at large $\Delta\eta$. Further clarification of the situation will require an increase in statistics.

4 Conclusions

We have explicitly demonstrated that the Tevatron data on the gaps-between-jets process at both 630 GeV and 1800 GeV are in broad agreement with the predictions obtained using the leading order BFKL formalism. However, we are not able to explain the behaviour of the CDF gap fraction at large $\Delta\eta$. Agreement is obtained

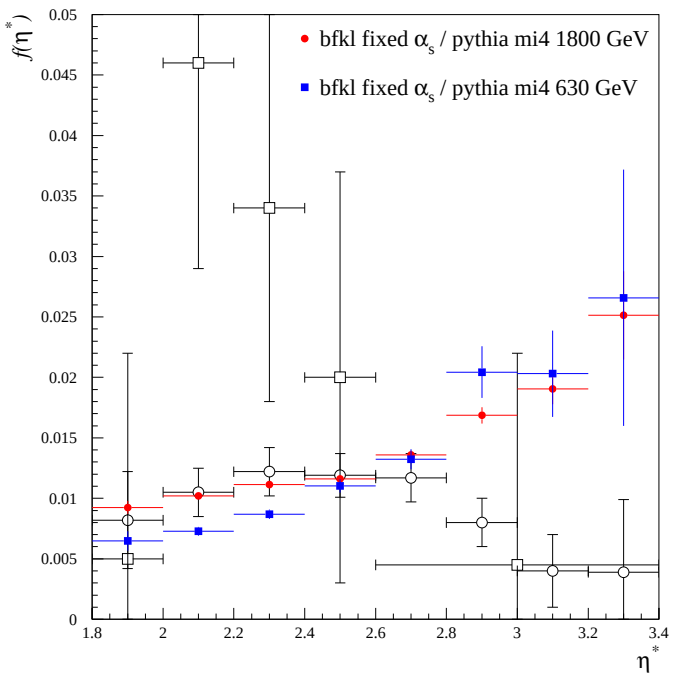

Figure 19: Gap fraction compared to the CDF data at 630 GeV (open squares) and 1800 GeV (open circles).

using the same fixed value of $\alpha_s = 0.17$ as was used to explain the recent HERA data on high-t double diffraction dissociation.

This agreement should be set in context. The theoretical formalism used does suffer from being evaluated only to leading logarithmic accuracy. There is an essentially unknown overall normalisation (due to the ambiguity in the choice of scale which defines the leading logarithms, i.e. the parameter c discussed in Section 3) and the procedure for determining the correct treatment of the running coupling is not defined. To improve upon these shortcomings requires an understanding of BFKL dynamics at non-zero t which goes beyond the leading logarithmic approximation.

Crucial in developing a description which is simultaneously consistent with the Tevatron data at 630 GeV and at 1800 GeV, and the HERA data at 200 GeV, is a realistic treatment of the soft underlying event and its impact on the survival of rapidity gaps. Using PYTHIA to model the underlying event we find an overall gap survival factor which is independent of the jet E_T and rapidity but dependent upon the overall centre-of-mass energy.

However, the gap fraction is not a very clean observable. We found very significant corrections from parton showering and hadronisation to both the colour-singlet

and non-colour singlet exchange processes which do not cancel on taking the ratio and which persist to the largest values of E_T. Moreover, the influence of the soft underlying event (which we accounted for using a multiple interactions model in PYTHIA), is also very significant at the smaller values of E_T, i.e. $E_T < 30$ GeV. A good understanding of the role of the underlying event for $E_T < 30$ GeV is therefore crucial in comparing with the data.

Acknowledgements

We should like to thank Andrew Brandt, Dino Goulianos, Mark Hayes, Mike Seymour and Torbjörn Sjöstrand for helpful discussions. This work was supported by the EU Fourth Framework Programme 'Training and Mobility of Researchers', Network 'Quantum Chromodynamics and the Deep Structure of Elementary Particles', contract FMRX-CT98-0194 (DG 12-MIHT). BC would like to thank the UK's Particle Physics and Astronomy Research Council for support.

References

[1] J. D. Bjorken, Phys. Rev. **D47** (1992) 101.

[2] A. H. Mueller and W. -K. Tang, Phys. Lett. **B284** (1992) 123.

[3] H1 Collaboration, "Double Diffraction Dissociation at large $|t|$ in Photoproduction at HERA", contribution to the 29th International Conference on High-Energy Physics ICHEP98, Vancouver, Canada, 1998;
B. E. Cox, "Double Diffraction Dissociation at large $|t|$ from H1", contribution to the DIS99 Workshop, Zeuthen, Germany (1999) `hep-ph/9906203`.

[4] S. Abachi et al (DØ Collaboration), Phys. Rev. Lett. **72** (1994) 2332; Phys. Rev. Lett. **76** (1996) 734.

[5] B. Abbott et al (DØ Collaboration), Phys. Lett. **B81** (1998) 189.

[6] F. Abe at al (CDF Collaboration), Phys. Rev. Lett. **74** (1995) 855;
Phys. Rev. Lett. **80** (1998) 1156.

[7] F. Abe at al (CDF Collaboration), Phys. Rev. Lett. **81** (1998) 5278.

[8] M. Derrick et al (ZEUS Collaboration), Phys. Lett. **B369** (1996) 55.

[9] H1 Collaboration, "Rapidity gaps between jets in Photoproduction at HERA", contribution to the International Europhysics Conference on High Energy Physics, Jerusalem, Israel (1997).

[10] H1 Collaboration, "Production of J/ψ Mesons with large $|t|$ at HERA", contribution to the International Europhysics Conference on High Energy Physics, Jerusalem, Israel (1997).

[11] J. Crittenden, "Recent Results from Decay-Angle Analyses of ρ^0 Photoproduction at High Momentum Transfer from ZEUS", contribution to the DIS99 Workshop, Zeuthen, Germany (1999) hep-ex/9906005.

[12] J.R. Forshaw and P.J. Sutton, Euro. Phys. J. **C14** (1998) 285.

[13] I. Balitsky and L.N. Lipatov, Sov. J. Nucl. Phys. 28 (1978) 822.

[14] J. R. Forshaw, "High-t Diffraction", contribution to the DIS99 Workshop, Zeuthen, Germany (1999) CERN-TH/99-143, hep-ph/9905557.

[15] PYTHIA version 6.127, program and manual,
T. Sjöstrand, Comput. Phys. Comm. **82** (1994) 74.
See also http://www.thep.lu.se/~torbjorn/Pythia.html.

[16] G. Marchesini et al, Comp. Phys. Comm. **67** (1992) 465.

[17] J. M. Butterworth, M. E. Hayes, M. H. Seymour and L. E. Sinclair, "Rapidity gaps between jets", in the proceedings of the Workshop 'Future Physics at HERA', eds. G. Ingelman, A. de Roeck and R. Klanner, DESY (1996).

[18] M. E. Hayes, University of Bristol PhD Thesis (1997).

[19] H. L. Lai et al, Phys. Rev. **D55** (1997) 1280.

[20] H. Plothow-Besch, "PDFLIB User's Manual", W5051 PDFLIB, 1997.07.02, CERN-PPE; Int. J. Mod. Phys. **A10** (1995) 2901.

[21] A. Donnachie and P. V. Landshoff, Z. Phys. **C2** (1979) 55, erratum-ibid **C2** (1979) 372; Phys. Lett. **B387** (1996) 637.

[22] S. J. Brodsky et al, "The QCD Pomeron with Optimal Renormalisation", SLAC-PUB-8037, IITAP-98-010, hep-ph/9901229.

[23] T. Sjöstrand and M. van Zijl, Phys. Rev. **D36** (1987) 2019

[24] J.M. Butterworth and R.J. Taylor, "A Global study of Photon Induced Jet Production", hep-ph/9907394, to be published in the proceedings of Photon '99, Freiburg, Germany (1999). See also http://www.hep.ucl.ac.uk/~jmb/HZTOOL/.

[25] B. Abbott et al (DØ Collaboration), Nucl. Instrum. Methods **A424** (1999) 352. See also http://www-d0.fnal.gov/~jkrane/approved_plots.

[26] S.D. Ellis, private communication to the OPAL Collaboration; D.E. Soper and H.-C. Yang, private communication to the OPAL Collaboration; L.A. del Pozo, University of Cambridge PhD thesis, RALT-002 (1993); R. Akers et al (OPAL Collaboration), Z. Phys. **C63** (1994) 197.

[27] F. Abe et al (CDF Collaboration), Phys. Rev. **D45** (1992) 1448.